J. Fluid Mech. (1986), *vol.* 166, *pp.* 379–407
Printed in Great Britain

Structure formation in bidisperse sedimentation

By G. K. BATCHELOR AND R. W. JANSE VAN RENSBURG
Department of Applied Mathematics and Theoretical Physics,
University of Cambridge

(Received 26 November 1984 and in revised form 7 October 1985)

It is known that when two different species of small particles with radii in the range 10–100 μm are dispersed uniformly in fluid and are settling under gravity, there may be a tendency for the particles of each species to gather together and develop a bulk vertical streaming motion, which results in much larger magnitudes of the mean velocity of at least one of the two types of particle. After a review of the published data on such streaming motions we describe new visual and photographic observations of the evolution of the internal structures (which are sometimes more globular than columnar) in a large number of different bidisperse systems. It appears that the observed structures result from instability of the statistically homogeneous dispersion to small concentration disturbances for certain combinations of values of the ratios of the sizes and densities of the two types of particle and the volume fractions of the two species.

The condition for growth of a sinusoidal disturbance of the homogeneous dispersion is derived from the two particle-conservation equations and is found to involve the dependence of the two mean particle velocities on the two particle concentrations in a homogeneous dispersion. Previously calculated values of these mean velocities for a dilute dispersion suggest that the condition for instability is indeed satisfied for not-too-small particle concentrations and certain combinations of the size and density ratios of the two particle species. The results of the instability theory are generally consistent with the observed features of the structures, regarded as finite-amplitude forms of the small disturbances with maximum growth rate.

1. Introduction

It was noticed by Whitmore (1955) that the effect of adding neutrally buoyant particles to a monodisperse system of small sedimenting spherical particles is to *increase* the settling speed of the heavy particles when the total volume fraction of the particles exceeds about 0.15, and that this increase in the settling speed is a consequence of the heavy particles gathering together in vertical columns and falling as a whole without being impeded by the neutrally buoyant particles. This appears to have been the first observation of the formation of internal structures in bidisperse sedimentation. The phenomenon was not investigated further until the work of Weiland and his co-workers (Weiland & McPherson 1979; Fessas & Weiland, 1981, 1982, 1984; Weiland, Fessas & Ramarao 1984), who found that streaming columns are formed over a wide range of properties of the two particle species. These authors point out the potential value to chemical engineers of a means of increasing particle settling speeds.

The formation of internal structures in an initially statistically homogeneous bidisperse system of sedimenting particles implies a rather remarkable spontaneous

local clustering and separation of the two particle species. Most of the previous papers have been concerned with the resulting increases in the mean velocities of one or both of the particle species, and the possible exploitation of these greater settling rates in practice. Our purpose however is to investigate the phenomenon of structure formation and to try to understand its origin. We have made new visual observations of structure formation with two general purposes, viz. (i) to illuminate the early stages of the process, and (ii) to explore the bounds on the values of the governing parameters for which internal structures form. We shall also present a theory of the instability of an initial well-mixed state in which a growing disturbance is simply a bidisperse form of the kind of concentration wave in a monodispersion first analysed by Kynch (1952). The condition for instability involves only the mean velocities of the two species of particle as functions of the concentrations of the two species in a homogeneous dispersion, about which a little information is available. The comparison between our observations and our theory that we shall make in §7 encourages the belief that the observed internal structures are a finite-amplitude form of these growing small disturbances.

2. Previous observations of streaming columns

The conditions under which streaming columns form have not previously been investigated directly, but some of the relevant facts can be inferred from the observations reported in the literature. We have listed in table 1 the properties of the particle pairs for which the existence of streamlining columns has been reported. (Fessas & Weiland 1984 say they have observed streaming columns with some other particle pairs but do not give the details needed for inclusion in table 1). It appears from the work of Weiland *et al.* (1984) that streaming columns may form when the velocities of isolated particles of the two species have either the same or different senses, although visual observations by these and other authors indicate that the streaming columns are more clearly defined for larger magnitudes of the relative velocity of isolated particles of the two species.

We give in the table the values of the Reynolds number of the flow about an isolated particle of one of the two species. The Reynolds numbers are all smaller than unity, much smaller in some cases, which indicates that inertia of the fluid has no effect on the properties of these statistically homogeneous dispersions; and since the particle densities are all comparable with that of the continuous fluid phase, particle inertia is likewise excluded. Furthermore, the values of the Péclet number, defined as $a_1 U_{10}/D_1$ (where $D_1 = kT/6\pi\mu a_1$ is the Brownian diffusivity of an isolated spherical particle of radius a_1), all exceed 10^7, showing that Brownian motion of the particles plays no part in the formation of internal structures.

It appears that a necessary condition for the formation of streaming columns is that the total volume fraction of the two types of particle should not be small. This is suggested by the observations of the steady-state settling speed of one type of particle as a function of the volume fractions of the two types made by Whitmore (1955) and Fessas & Weiland (1981, 1984) for the systems indicated under their names in table 1. At small total volume fraction each particle species apparently hinders the settling of the other in the general way that is expected when the dispersion is statistically homogeneous (and for which accurate numerical results have recently been calculated by Batchelor & Wen 1982). But as the total particle volume fraction is increased above about 0.15 the mean speed of each particle species begins to rise,

	Whitmore (1955)	Weiland & McPherson (1979)	Fessas & Weiland (1981)	Weiland *et al.* (1984) A	Weiland *et al.* (1984) B	Weiland *et al.* (1984) C	Fessas & Weiland (1984) A	Fessas & Weiland (1984) B
				Fluid				
ρ_0 gm/cm^3	1.056	1.10	2.24	1.124	1.062	1.124	1.586	2.242
μ gm/cm s	0.0105	0.0193	0.0209	0.0495	0.0180	0.0495	0.0152	0.0209
				Particles of type 1				
$\rho_1-\rho_0$ gm/cm^3	0.132	0.28	0.72	0.282	1.401	0.282	0.916	0.718
a_1 mm	0.048	0.100	0.050	0.069	0.045	0.109	0.024	0.058
U_{10} mm/s	0.63	3.16	1.88	0.59	3.44	1.48	0.77	2.47
$\frac{a_1 U_{10}\rho_0}{\mu}$	0.032	0.80	0.101	0.0092	0.091	0.037	0.019	0.152
ϕ_1	Various	Various	Various	0.175	0.175	0.143	Various	Various
				Particles of type 2				
$\frac{\rho_2-\rho_0}{\rho_1-\rho_0}(=\gamma)$	0	−0.21	−1.17	−1.88	0.246	1.0	−0.197	−1.170
$\frac{a_2}{a_1}(=\lambda)$	1.02	1.0	1.08	1.0	1.0	0.63	2.02	1.00
ϕ_2	Various	Various	Various	0.165	0.175	0.095	Various	Various

TABLE 1. Bidisperse systems of approximately spherical rigid particles in which streaming columns have previously been observed. The particle radius a_i is an average value, with about 10% standard deviation in most cases. U_{i0} is the vertical component of the velocity (positive downward) of an isolated type-i particle calculated from Stokes's law. ϕ_i is the fraction of the total volume occupied by particles of type i in the initial well-mixed dispersion.

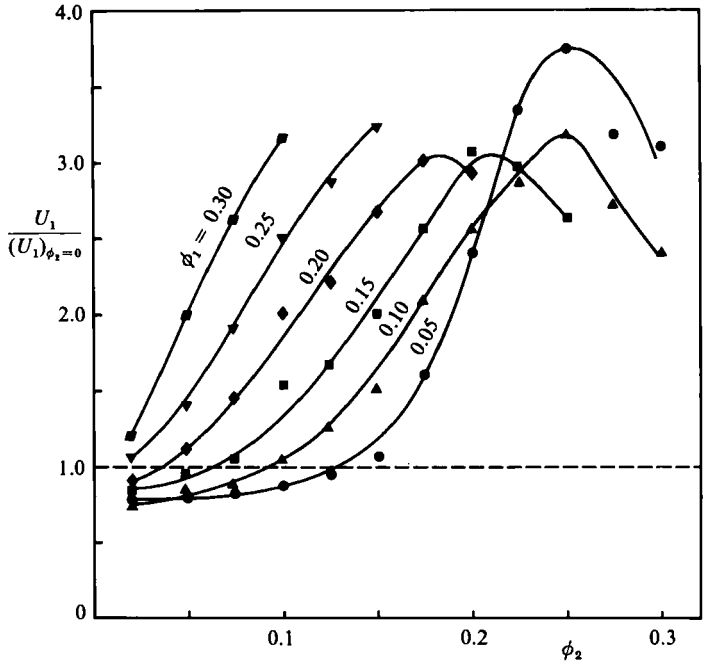

FIGURE 1. The dependence of the mean fall speed of (heavy) particles on the concentration of a second species of (buoyant) particles, as observed by Fessas & Weiland (1981).

and may attain a value many times larger than that in the complete absence of the other species before beginning to fall again when the total particle volume fraction reaches about 0.40. Figure 1 taken from Fessas & Weiland (1981) shows some of the measurements of mean particle speeds made by these authors.

The form of the internal structures that appear spontaneously in a homogeneous bidispersion of sedimenting particles is difficult to observe and is less well documented than the resulting changes in mean velocity of each species. Weiland and co-workers refer to 'lateral separation' of the two species and to the formation of vertical fingers or columns in which one of the two species is concentrated and which develop a vertical gravity-driven bulk motion. Fessas & Weiland (1984) describe the observed internal structures as vertical streaming columns '3.5 mm in diameter containing the less populous species' which 'form and flow through a concentrated continuum suspension of the more populous species'. Weiland *et al.* (1984) also report that there is a preferred width of the streaming columns at any instant, and that there appears to be a gradual decrease of this characteristic width yielding columns 'of increasingly finer scale'. The only published photographs of bidisperse sedimenting particles which reveal the distribution of the separate species are those taken by Weiland *et al.* (1984). They show one photograph for each of the systems B and C listed under their names in table 1, and a sequence of small photographs of their system A at 10 s intervals.

Many questions concerning the origin of internal structures remain open. There is in particular a lack of information about their growth and form in the early stage prior to the development of bulk vertical motions due to appreciable spatial variations of particle concentration. Nor is there any information about critical conditions for the formation of structures. The authors mentioned above report the

Particle species	Radius (mm)	Density (gm/cm^3)	Material
I	0.24 ± 0.02	1.175 ± 0.001	Acrylic
II	0.24 ± 0.02	1.049 ± 0.001	Polystyrene
III	0.16 ± 0.02	1.175 ± 0.001	Acrylic
IV	0.16 ± 0.02	1.051 ± 0.001	Polystyrene
V	0.41 ± 0.04	1.047 ± 0.001	Polystyrene
VI	0.40 ± 0.04	1.043 ± 0.001	Polystyrene
VII	0.24 ± 0.02	1.039 ± 0.001	Polystyrene
VIII	0.37 ± 0.03	1.0395 ± 0.0005	Polystyrene
IX	0.16 ± 0.01	1.0440 ± 0.0005	Polystyrene
X	0.31 ± 0.02	1.0395 ± 0.0005	Polystyrene
XI	0.24 ± 0.02	1.0450 ± 0.0005	Polystyrene
XII	0.41 ± 0.04	1.0475 ± 0.0005	Polystyrene

TABLE 2. Physical properties of the particles used in the experiments.

existence of structures and bulk convective motions in every bidisperse system they studied except ones for which either of the two particle volume fractions is very small, but it seems intrinsically likely that there are other conditions for their existence.†

3. New observations of the formation of structures

A primary purpose of our observations was to determine the conditions under which structures form spontaneously in the interior of a homogeneous bidispersion of sedimenting spherical particles. Each bidisperse system requires the values of four parameters for its specification, namely the ratios of the radii and of the (reduced) densities of the two species,

$$\lambda = \frac{a_2}{a_1}, \quad \gamma = \frac{\rho_2 - \rho_0}{\rho_1 - \rho_0},$$

and the volume fractions of the two species in the homogeneous dispersion, ϕ_1 and ϕ_2. In order to get some idea of the systematic dependence of the behaviour of a system on these parameters we made most of our observations on two sets of systems, in each of which two of the parameters were kept constant. For the systems in the first set $\lambda \approx 1$, $\gamma \approx -1$, and the concentrations ϕ_1 and ϕ_2 were varied; and for those in the second set $\phi_1 = \phi_2 = 0.15$, and the particle properties λ and γ were varied.

The particles used were polystyrene and acrylic spheres of various sizes and densities (some dyed), and their properties are listed in table 2. Each species in the table, labelled by a Roman numeral, was obtained by sieving particles into the size range quoted and then separating them into the stated density range by alternately sinking and floating in liquids of known density (at a constant temperature of 19.5 °C).

† Whitmore (1955) even says that 'vertical currents' are 'present to a small extent' in a monodispersion (of his type 1 spheres described in table 1), although neither we nor Weiland & McPherson (1979) find evidence of sustained bulk vertical motions when particles of uniform radius in the range 10–100 μm are dispersed in liquid. It is of course to be expected that in any dispersion there will be fluctuations in the number of particles instantaneously lying within a region of specified volume and that when this fluctuation is large there will be bulk convection and instantaneously an above-average vertical speed of all the particles in this region. Such collective motions are transient, but are not easily distinguished from a weak systematic development of structures of the kind observed in some bidispersions.

System	A	B	C
Particle type 1	I	IV	VI
Particle type 2	II	III	V
ρ_0(gm/cm^3)	1.112	1.113	1.045
μ(cP)	4.70	4.95	1.70
U_{10} (mm/s)	1.61	0.70	0.41
$a_1 U_{10}\rho_0/\mu$	0.09	0.03	0.11
λ	1.0	1.0	1.03
γ	−1.0	−1.0	−1.0

TABLE 3. The three systems for which $\lambda \approx 1$, $\gamma \approx -1$.

The suspending liquid was an aqueous glycerol solution to which a few drops of liquid detergent had been added to prevent the particles from sticking together. With one exception (system B in table 3), the dispersions we observed were all contained in a rectangular clear Perspex cell 20 cm tall, 10 cm wide and with a gap width of 5 mm between the parallel plates. The cell used in B was 37.5 cm tall, 5 cm wide with a gap of 3 mm.

A small quantity of lead shot (2 mm in diameter) was added to the contents of the cell to facilitate mixing, and as much as possible of the trapped air was removed before it was sealed. Mixing required some dexterity in practice and was done by first holding the cell vertical and rapidly rotating it in its own plane about its centre to dislodge the sedimented beds and then inverting it many times using the shot to homogenize the mixture. In the final stages it was also shaken from side to side during the downward passage of the shot to prevent any possible vertical structure remaining in their wake. All the while the contents were kept under scrutiny by back-lighting the cell. When it was judged by eye to be uniformly mixed, the cell was quickly placed in a photographic rig and photographed under back-lighting.

The random nature of the emerging structures makes it extremely difficult to obtain reliable quantitative information. The results that follow are based on impressions gained by comparing photographic sequences as well as from direct visual observation.

Systems for which $\lambda \approx 1$, $\gamma \approx -1$

In these systems the particles are equally and oppositely buoyant with respect to the suspending fluid, the symmetry being broken only if the volume fractions of the two particle species are different. The end state of these systems consists of packed beds at the upper and lower boundaries of the cell which contain exclusively one kind of particle or the other and whose depths are proportional to the initial volume fractions of their respective particles.

Table 3 lists the physical parameters of the three systems (designated as A, B and C) with pairs of particle species for which $\lambda \approx 1$, $\gamma \approx -1$. Table 4 gives the volume fractions in the systems observed and summarizes the impressions gained of their behaviour. The entries in the column headed 'stability' indicate that the particular system was judged to be stable (designated 'S'), unstable ('U') or, being undecidable, marginal ('M').

All those systems classed as unstable acquired a 'grainy' appearance within a few seconds of the cessation of mixing, the intensity being stronger in some cases than in others. As illustrated in figure 2(*a*) (system A11 at 2 s), these 'grains' are small

System	ϕ_1	ϕ_2	Stability	Type	Contrast	d/a_1	$\tau \lvert U_{10} \rvert / a_1$
A 1	0.30	0.14	U	B	G	67	60
2	0.30	0.08	U	B	G^-	33	47
3	0.30	0.04	U	B	F	21	40
4	0.30	0.025	M	—	—	—	—
5	0.30	0.016	S	—	—	—	—
6	0.30	< 0.01	S	—	—	—	—
7	0.26	0.19	U	B	G^+	63	74
8	0.25	0.15	U	B	G	54	74
9	0.25	0.07	U	BC	F^-	29	60
10	0.25	0.02	S	—	—	—	—
11	0.20	0.20	U	BC	G	54	60
12	0.20	0.14	U	CB	F	46	47
13	0.20	0.09	U	CB	P^+	29	34
14	0.20	0.03	S	—	—	—	—
15	0.16	0.16	U	C	P^+	31	34
16	0.16	0.10	U	C	P^+	25	34
17	0.16	0.06	M	C	—	—	—
18	0.13	0.12	U	C	P^-	25	?
19	0.12	0.12	U	C	P^+	25	34
20	0.12	0.12	U	C	P	25	20
21	0.13	0.07	M	C	—	—	—
22	0.12	0.06	M	C	—	—	—
23	0.12	0.03	S	—	—	—	—
24	0.12	0.025	S	—	—	—	—
25	0.11	0.11	U	C	P^-	21	20
26	0.10	0.10	U	C	P^-	21	20
27	0.08	0.08	M	C	—	—	—
28	0.07	0.07	S	—	—	—	—
B 1	0.15	0.15	U	CB	F	31	39
2	0.25	0.08	U	CB	F	31	48
C 1	0.15	0.15	U	BC	G^-	50	> 62
2	0.21	0.15	U	B	G^+	50	> 62

TABLE 4. The observed features of the structures formed in systems for which $\lambda \approx 1$, $\gamma \approx -1$.

irregular regions, several particle radii across, in which there appears to be more of one particle species than the other, but whose boundaries proved to be impossible to locate with any certainty, especially in the weakly unstable systems. They were randomly and homogeneously distributed over the cell when it was well mixed.

Initially only individual particle motions could be seen. But as the excess number of particles of one species in some small region increases, so does the effective buoyancy of this region, and eventually convective motion is generated by the excess buoyancy and groups of particles move as a whole. Figures 2 (*a*)–(*e*) show photographs at stages in the development of system A11 up to the time when fairly large structures have formed, and figure 2 (*c*) (at 8 s) illustrates the beginning of the period during which convective motion spreads throughout the cell.

The convective structures which evolved in the various systems are designated in table 4 as being of one of the following types:

Type B: 'Blobs', distinct self-contained buoyant or heavy regions rising or falling coherently as drops with only minor skirts or tails and generally containing only the species that was in the minority in systems in which ϕ_1 and ϕ_2 are large and unequal.

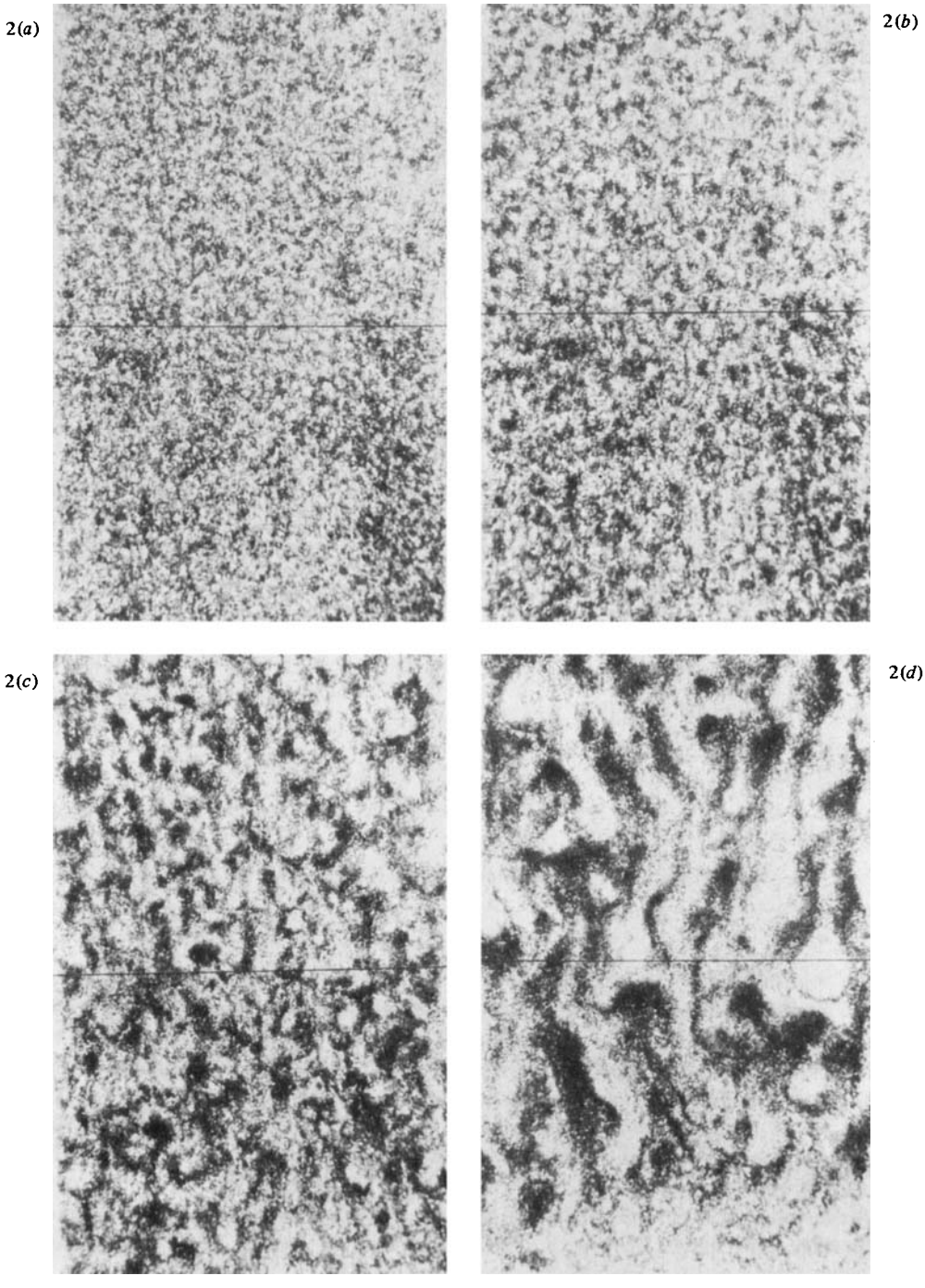

FIGURE 2. System A11, with structures classified as blobs with tails and good contrast. The horizontal width of the portion of the cell in the photographs is 10 cm. (*a*) At 2 s, (*b*) 4 s, (*c*) 8 s, (*d*) 16 s, and (*e*) 24 s.

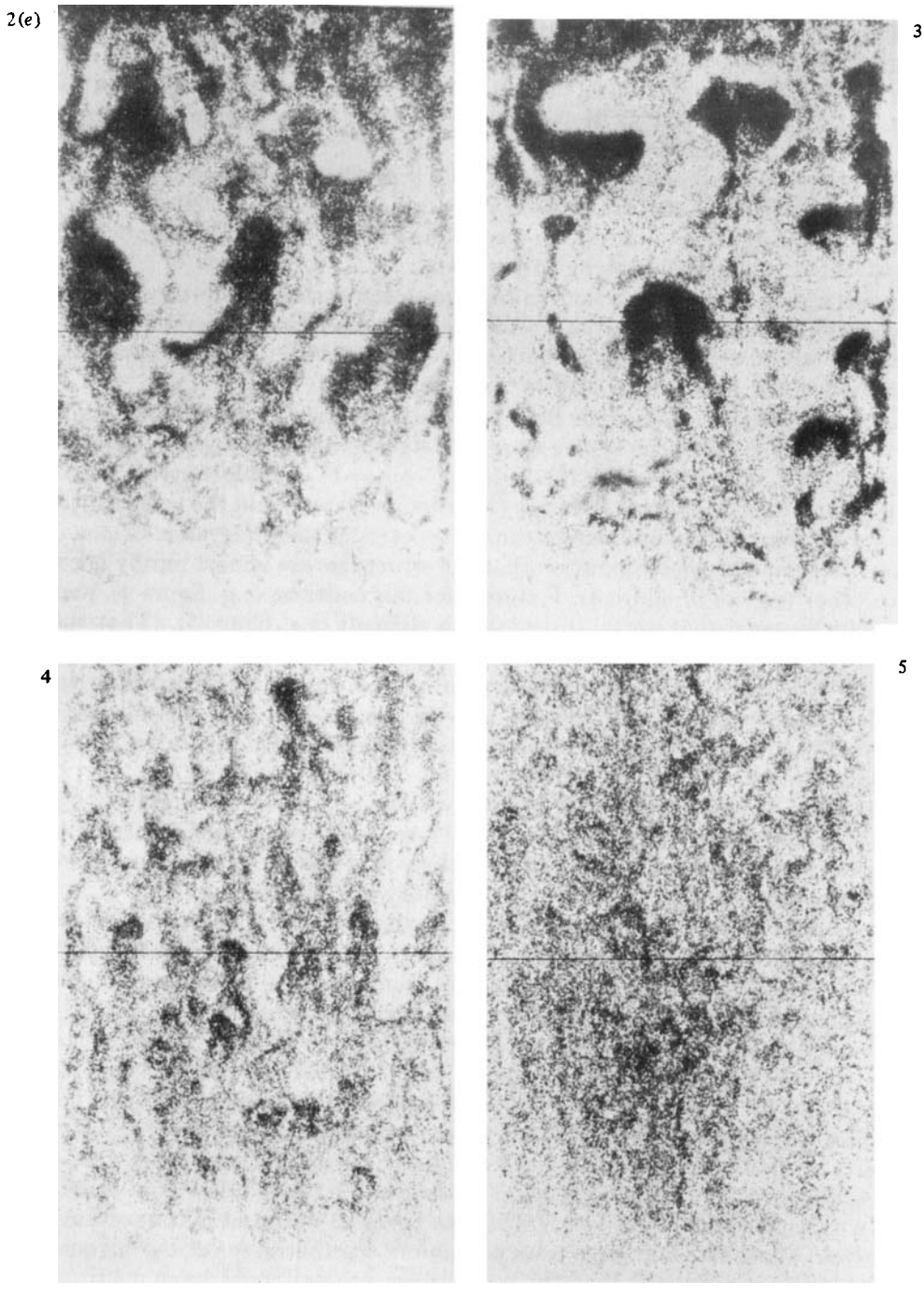

FIGURE 2(*e*). For caption see facing page.

FIGURE 3. System A1 at 22 s, with structures classified as blobs with good contrast.

FIGURE 4. System A15 at 20 s, with structures classified as streaming columns with head formation and fair contrast.

FIGURE 5. System A16 at 20 s, with structures classified as streaming columns with poor contrast.

An example is shown in figure 3 (system A1 at 22 s). These objects grow by coalescence to fairly large sizes and did not appear to have completed their evolution before merging with the packed beds at the ends of the cell.

Type BC: Similar to the above but with more pronounced tails or skirts, illustrated in figure 2(*e*) (system A11 at 24 s). These occur in systems in which the two volume fractions are large and nearly equal.

Type CB: Streaming columns, i.e. coherent vertically flowing regions, which showed a tendency to form heads, illustrated in figure 4 (system A15 at 20 s).

Type C: Streaming columns, often meandering irregularly, with no noticeable head formation, as in figure 5 (system A16 at 20 s).

In every case the stronger and more intense structures precipitated out first (at between 30–60 s) after which the activity in the cell declined as smaller and smaller features followed until only single particles remained, the process culminating in the separation of the two species (within 2 minutes).

The type 1 particles in particle pair A defined in table 3 were virtually transparent acrylic (species I) while the type 2 were polystyrene dyed dark red (species II). The designations P, F and G under the heading 'contrast' in table 4 give an indication of the photographic contrast between the principal features in the cell and therefore reveal something of the mixture of the two species in these features. G means good contrast and such strong separation that the structures are almost purely one species or the other (e.g. as in figure 3), F stands for fair contrast (e.g. figure 4), and P for such poor contrast that visual distinction is difficult (e.g. figure 5). (That there are streams present in these latter cases is more evident to the naked eye which detects them by their motion.) It also appears from the photographic record that the same contrast classifications apply quite closely throughout each time sequence, which supports the notion that particle separation occurs essentially only in the initial phase and is not greatly affected by the subsequent convective motion.

The time τ at which convective motion was estimated by eye to have set in over most of the cell is given in non-dimensional form in the last column in table 4. Since bulk convection did not develop simultaneously in all parts of the cell, most probably due to imperfect mixing, there is an uncertainty in τ of about $\pm 15\,\%$.

The column in table 4 headed d/a_1 gives an estimate of the (non-dimensional) horizontal widths of the structures composed mainly of the dyed particles (type 2, almost always having the smaller volume fraction). This estimate was made for convenience at the same time in every case, viz. 20 s after the cessation of mixing (corresponding to a non-dimensional time 134), by which time the structures had developed into their characteristic types. In particular, the 'blob' types had had sufficient time to grow by coalescence from smaller blobs, beginning with the grains produced by the instability. It was noticed that increasing ϕ_2 at a given value of $\phi_1 (> \phi_2)$, as in the sequences A3, A2, A1 and A9, A8, A7 and A13, A12, A11 in table 4, gave rise to improved particle separation and blobs that grew increasingly rapidly by coalescence in the interval of time between the onset of convection (τ) and the instant at which their sizes were estimated. Furthermore, at the higher values of ϕ_2 at least, it appeared that the coalescence process could have continued and produced even larger blobs had the process not been limited by the size of the cell. On the other hand, convective motion developed sooner in systems producing columns than in those producing blobs, and partly for this reason it was difficult to discern the process by which the columns developed. However, at the time their sizes were estimated they appeared to have steady average horizontal widths. They

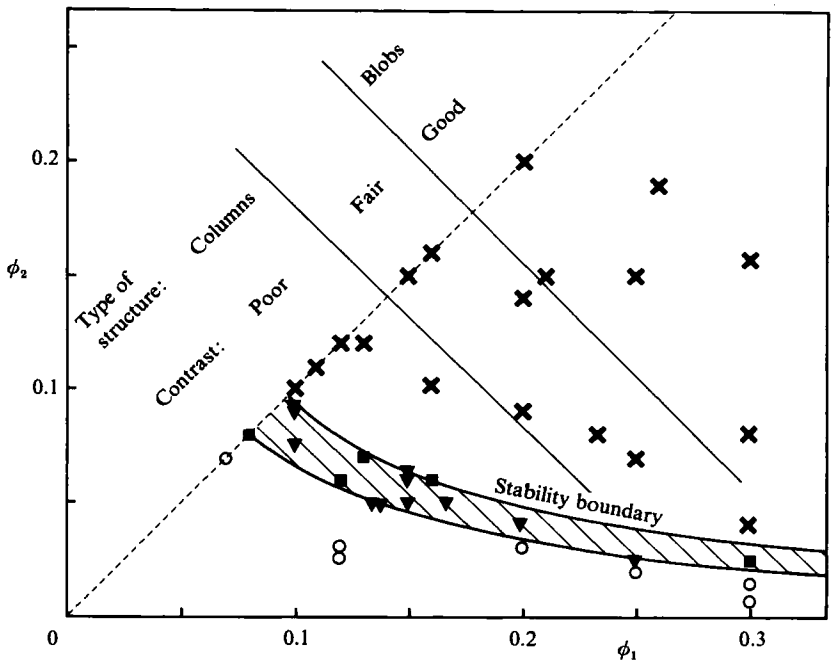

FIGURE 6. The stability of systems for which $\lambda \approx 1$, $\gamma \approx -1$ as a function of ϕ_1 and ϕ_2. ×, system classified as unstable; ■, marginally unstable; ○, stable. ▼ denotes a system observed by Fessas & Weiland (1981, 1984) to be marginally unstable in the sense that there was a small increase in the mean velocity of at least one species.

exhibited a range of vertical lengths which proved impossible to quantify beyond the simple observation of being several times larger than their horizontal widths.

The above observations of unstable systems allow the following generalizations: the higher the initial total volume fraction the more likely the system is to form blobs with good particle separation and the longer it takes for convective motion to become established; and low-volume-fraction systems which are unstable tend to form streaming columns with poor particle separation and approximately constant horizontal dimensions.

Finally, in those systems classified in table 4 as stable, no coherent convective structures arose and, although continuous small-scale cluster formation and breakup was observed in some cases, the definite 'graininess' of a fully unstable system did not occur. The stability characteristics of those systems classified as 'marginal' were unclear; they showed scattered and transient graininess, with poor contrast, but this did not lead to any definite flow structure although it may have raised the mean sedimentation velocities of the species concerned a little.

All these results are summarized in figure 6. Note that the stability of a system for which $\lambda = 1$, $\gamma = -1$ must be invariant under the exchange of ϕ_1 and ϕ_2 so that only half a quadrant of the (ϕ_1, ϕ_2)-plane need be considered. The band shown in figure 6 contains all the systems that are marginal and defines reasonably well a stability boundary.

It is possible at this point to make a rough comparison of the above observations of critical conditions with those made by Fessas & Weiland (1981, 1984) on systems

for which $\lambda \approx 1, \gamma \approx -1$ (viz. those described in the 3rd and 8th columns of table 1). Fessas & Weiland measured the mean velocities of the two types of particle, an example of their results being shown in figure 1, and did not otherwise observe the instability of the individual systems. However, since the *increase* in the magnitude of the mean sedimentation velocity of one species which results from the presence of the other species is presumably a consequence of the existence of convective structures in these systems, it is possible to infer something of their stability from these results. In particular, if the ratio of the mean sedimentation velocity of one of the species in the bidisperse system to the mean sedimentation velocity of the same species in a monodisperse system at the same volume fraction is greater than one, then the system is evidently unstable. We find that all the systems for which Fessas & Weiland report this ratio to exceed one lie in the part of figure 6 that corresponds to unstable systems. The solid triangles in figure 6 represent systems for which Fessas & Weiland find that the ratio is approximately unity (as indicated by curves like those shown in figure 1), and it is reassuring, in view of the difference between the two measures of instability, that all these points lie within our marginal-stability band.

Systems for which $\phi_1 = \phi_2 = 0.15$

In these experiments both particle species were made of polystyrene, although with differing densities. A range of values of γ was obtained by adjusting the density of the suspending fluid which again was an aqueous glycerol solution. $|\gamma|$ is restricted to lie between 0 and 1 by the convention that the species called type 1 (the reference species) was that whose density differed more from that of the fluid. The few systems for which γ lies between -1 and 0 were obtained by using a fluid whose density lay between those of the particles.

When γ is positive, as it is for most of these systems, both types of particles sediment in the same direction, a circumstance which makes the behaviour of these systems more subtle and produces in them a greater variety of end states than those for which $\gamma < 0$. The single packed bed which forms at one end of the cell may be divided into two major zones. The zone further from the boundary consists exclusively of the particles whose free-fall speed is the smaller and its depth depends partly, at least in stable systems, on the relative fall speeds of the two particles. In contrast, the zone adjacent to the boundary exhibits a number of possible states, ranging from homogeneous mixtures of the two species in systems which are stable, to stratified layers resulting from the deposition of varying mixtures of particles at different stages in the development in time of an unstable system. Unfortunately the existence of this stratification is not always manifest, especially in weakly unstable systems, and this reduces its value as an indicator of the existence of the instability itself. The composition of the packed beds is one of many aspects of the convective structures which might have practical significance.

Table 5 lists the parameters of the systems for which $\phi_1 = \phi_2 = 0.15$ and the observations made on them. The stability classifications have the same meaning as before but, owing to the wide range of opaque, tinted and dyed particles used, the contrast classification is much more subjective.

Generally speaking, and ignoring considerations of the motions of the concentration fronts in the cell, the time development of the unstable systems for which $\gamma > 0$ follows the same pattern as that previously described for cases in which $\gamma = -1$. That is, after the cessation of mixing a similar 'graininess' develops followed by the onset of bulk convection and its evolution into large-scale structures. From the experimental point of view, however, there are certain differences which make precise observations

λ	γ	μ(cP)	Stab.	Cont.
	Type 1 = XII, type 2 = IX			
0.38	0.0	1.68	M	—
	0.075	1.67	M	—
	0.18	1.67	M	—
	0.33	1.63	M	—
	0.43	1.62	M	—
	0.56	1.60	S	—
	0.69	1.51	S	-
	0.79	1.43	S	—
	Type 1 = V, type 2 = IV			
0.39	0.0	1.85	M	—
	0.20	1.87	M	—
	0.33	1.90	S	—
	Type 1 = VI, type 2 = IV			
0.41	0.0	1.85	U	F^-
	0.27	1.93	U	F^-
	0.50	2.05	M	—
	0.79	2.78	S	—
	0.95	31.6	S	—
	Type 1 = XII, type 2 = XI			
0.57	−0.67	1.74	U	F
	−0.25	1.73	U	F
	0.29	1.68	U	F
	0.44	1.67	M	—
	0.71	1.60	S	—
	0.87	1.38	S	—
	0.95	1.15	S	—
	Type 1 = V, type 2 = VII			
0.57	0.0	1.60	U	F^-
	0.27	1.53	U	P
	0.53	1.43	M	—
	0.70	1.25	S	—
	0.83	1.15	S	—
	Type 1 = VI, type 2 = VII			
0.60	0.0	1.60	U	?
	0.20	1.57	U	?
	0.33	1.53	U	F^-
	0.56	1.50	M	—
	0.69	1.43	S	—
	0.82	1.25	S	—
	0.91	1.15	S	—
	Type 1 = V, type 2 = X			
0.76	0.	1.60	U	G
	0.11	1.57	U	F
	0.27	1.53	U	F^-
	0.38	1.50	U	P^+
	0.58	1.38	M	—
	0.83	1.15	S	—
	Type 1 = XII, type 2 = VIII			
0.90	0.0	1.59	U	F^+
	0.30	1.53	U	F
	0.41	1.50	U	F^-
	0.57	1.42	M	—
	0.70	1.28	M	—
	0.83	1.15	S	—
	Type 1 = V, type 2 = VI			
0.96	0.0	1.67	U	F^-
	0.33	1.62	U	F^-
	0.43	1.60	U	F^-
	0.85	1.26	M	—
	0.92	1.15	S	—
	Type 1 = VI, type 2 = V			
1.04	−1.0	1.70	U	G^-
	0.0	1.75	U	F
	0.5	1.85	U	P
	0.67	1.95	M	P^-
	Type 1 = VIII, type 2 = XII			
1.11	0.0	1.75	U	F^+
	0.45	1.93	U	P^+
	0.57	2.02	M	—
	0.71	2.28	M	—
	0.81	2.83	S	—
	0.95	44.8	S	—
	Type 1 = X, type 2 = V			
1.32	0.0	1.75	U	F^+
	0.53	1.95	U	P^+
	0.62	2.05	M	—
	0.95	59.9	S	—
	Type 1 = VII, type 2 = VI			
1.68	0.0	1.67	U	F^+
	0.33	1.71	U	P^+
	0.50	1.75	M	—
	0.64	1.83	S	—
	0.81	2.05	S	—
	0.93	3.82	S	—
	Type 1 = VII, type 2 = V			
1.75	0.0	1.75	U	F
	0.33	1.85	U	P^+
	0.5	1.95	M	—
	0.62	2.05	M	—
	0.95	59.9	S	—
	Type 1 = XI, type 2 = XII			
1.75	−0.67	1.74	U	F^+
	0.0	1.75	U	F^-
	0.17	1.77	U	F^-
	0.29	1.78	U	P^+
	0.37	1.79	U	P^-
	0.50	1.83	M	—
	0.58	1.85	M	—
	0.64	1.87	S	—
	0.78	1.95	S	—
	0.94	3.22	S	—
	Type 1 = IV, type 2 = VI			
2.47	0.0	1.67	U	F^+
	0.47	1.53	M	—
	0.60	1.44	S	—
	0.72	1.29	S	—
	0.84	1.15	S	—
	Type 1 = IV, type 2 = V			
2.56	0.0	1.75	U	P^-
	0.33	1.71	M	—
	0.43	1.68	M	—
	0.64	1.60	S	—
	0.81	1.43	S	—
	0.87	1.25	S	—
	0.92	1.15	S	—
	Type 1 = IX, type 2 = XII			
2.65	−0.68	1.74	U	P^+
	−0.16	1.75	U	P^-
	0.0	1.76	M	—
	0.12	1.77	M	—
	0.35	1.81	S	—
	0.49	1.85	S	—
	0.81	2.16	S	—

TABLE 5. Observations of systems for which $\phi_1 = \phi_2 = 0.15$.

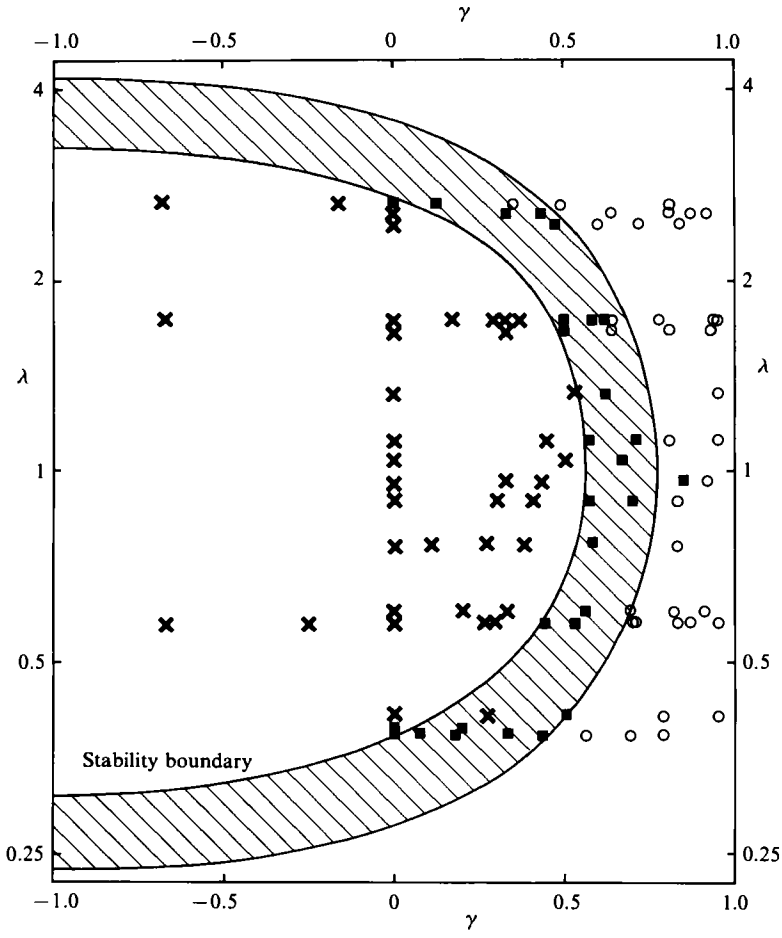

FIGURE 7. The stability of systems for which $\phi_1 = \phi_2 = 0.15$ as a function of λ and γ. ×, system classified as unstable; ■, marginally unstable; ○, stable.

even more elusive when $\gamma > 0$. In particular, the grains themselves were often noticeably in motion right from the start, and invariably very weakly formed, making the determination of the time of onset of convection virtually impossible in all but a few cases. Also, whereas in the $\gamma = -1$ systems the active zone in which convective structures exist vanishes at the time of separation of the two species, usually under 2 min in the systems studied, here the active zone vanishes when the trailing concentration jump of the faster-moving particle reaches the packed bed, at a time which was found to range from 45 s to nearly an hour, averaging about 10 min. These factors necessitated some repetition and refinement in order to determine whether a given system was stable or not.

Figure 7 shows the observed stability as a function of λ and γ. We have drawn a band containing the marginally stable systems, and its speculative extrapolations into the region where $-1 < \gamma < 0$. It appears that the band is approximately symmetrical about the horizontal line $\lambda = 1$. We know of no reason to expect this symmetry to be exact, although owing to the invariance of these systems under the interchange $\gamma \to 1/\gamma$, $\lambda \to 1/\lambda$, the stability boundary must cut the line $\gamma = -1$ at points equidistant from $\lambda = 1$ and with parallel tangents at these two points.

A last general inference from table 5 is that the strength of the convective structures resulting from the instability, as measured by their contrast, decreased as γ was increased with λ fixed, becoming zero at the stability boundary.

Again a comparison can be made with previously published results for some of the systems listed in table 1. Whitmore (1955) reported the existence of convective structures for the system $\lambda = 1.02$, $\gamma = 0$, $\phi_1 = \phi_2 = 0.15$, and so too did Weiland *et al.* (1984) for the system $\lambda = 0.63$, $\gamma = 1.0$, $\phi_1 = \phi_2 = 0.15$. Both these systems lie within the region in figure 7 that we find to correspond to unstable conditions. On the other hand, Weiland *et al.* (1984) reproduce a photograph showing the existence of rather faint columnar structures for the system $\lambda = 0.63$, $\gamma = 1.0$, $\phi_1 = 0.143$, $\phi_2 = 0.095$ (their system C in table 1), which does not seem to be consistent with our figure 7. Leaving aside the effect of the volume fractions in their system being a little smaller, the point in the (λ, γ)-plane corresponding to their system C lies in the stable region of figure 7. We do not know the reason for this apparent discrepancy.

4. Instability of a homogeneous bidisperse system to small disturbances

In seeking an explanation of the formation of internal structures we begin with the natural inference from the observations that a statistically homogeneous bidisperse sedimenting system is unstable to small disturbances. This is different from the more familiar kind of instability in which a small disturbance to a fluid motion or a boundary shape grows in magnitude, for here the particles have random positions and the state of the system is defined only statistically. We shall consider theoretically the response of the homogeneous system to perturbations of the concentrations of the two types of particle (represented by their volume fractions ϕ_1 and ϕ_2).

In the absence of an obvious physical mechanism of instability it seems appropriate to proceed initially on the simplest basis, and to begin with the approximate average form of the equation expressing conservation of particles of type i, viz.

$$\frac{\partial \phi_i}{\partial t} = -\nabla \cdot \{\phi_i (\boldsymbol{V} + \boldsymbol{U}_i)\} \quad (i = 1, 2), \tag{4.1}$$

where $\boldsymbol{V}$ is the local mean velocity of the mixture relative to the container walls and $\boldsymbol{U}_i$ is a mean velocity of particles of type i relative to local zero-volume-flux axes. Equation (4.1) is in error only inasmuch as contributions to the transport of particles due to fluctuations in the particle velocity are ignored. In an approximately homogeneous dispersion the effect of these velocity fluctuations, which may arise from Brownian motion if the particles are sufficiently small (of about one micron in diameter or less) and from hydrodynamic interaction with neighbouring particles, is to require the addition of a diffusion term

$$\sum_{j=1}^{2} \nabla \cdot (\boldsymbol{D}_{ij} \cdot \nabla \phi_j) \tag{4.2}$$

to the right-hand side of (4.1), provided the lengthscale of the spatial variation in ϕ_j is large compared with the particle size. The higher-order spatial derivative in (4.2) ensures that the diffusion term is negligible for sufficiently slow spatial variations of ϕ_j, and later we shall check that the diffusion term is indeed small for the spatial variations of ϕ_j that are found to be relevant.

In its more familiar monodisperse form equation (4.1) is the basis of the theory

of vertically propagating concentration waves of small amplitude initiated by Kynch (1952). In that theory it is customary to assume that the mean particle velocity relative to local zero-volume-flux axes is the same function of the local concentration as in a homogeneous dispersion, and we shall assume similarly that $\boldsymbol{U}_1$ and $\boldsymbol{U}_2$ depend only on the local values of ϕ_1 and ϕ_2. This assumption is evidently valid for sufficiently small spatial gradients of ϕ_1 and ϕ_2. Later we shall need to make a quantitative estimate of the conditions for validity

The mean mixture velocity $\boldsymbol{V}$, which is the only quantity in (4.1) not determined by ϕ_1 and ϕ_2 and the particle properties, in general must be found from an equation of motion of the mixture. However, $\boldsymbol{V} = 0$ in the statistically homogeneous dispersion and $\boldsymbol{V}\cdot\boldsymbol{\nabla}\phi_1$ is of second order in the perturbation quantities, so $\boldsymbol{V}$ does not enter into the analysis of stability of the homogeneous dispersion. The two equations represented by (4.1) are consequently sufficient for the determination of the perturbations in ϕ_1 and ϕ_2.

The linearized form of (4.1) for a small disturbance to the homogeneous dispersion is then

$$\frac{\partial \phi_i}{\partial t} = -\sum_{j=1}^{2}\left(\frac{\partial \phi_i \boldsymbol{U}_i}{\partial \phi_j}\right)^{(0)}\cdot\boldsymbol{\nabla}\phi_j \quad (i = 1,2), \tag{4.3}$$

where the superscript (0) indicates the value appropriate to the undisturbed dispersion. We now investigate the evolution of a disturbed state of the form

$$\phi_i = \phi_i^{(0)} + A_i \exp[\sigma t + \mathrm{i}\boldsymbol{k}\cdot(\boldsymbol{x} - \boldsymbol{c}t)] \quad (i = 1,2), \tag{4.4}$$

where σ, $\boldsymbol{k}$ and $\boldsymbol{c}$ are real, on the understanding that a perturbation of arbitrary initial form can be represented as a sum or integral of such three-dimensional Fourier components evolving independently. Substitution of (4.4) in (4.3) gives

$$(\sigma - \mathrm{i}\boldsymbol{k}\cdot\boldsymbol{c})\,A_i = -\mathrm{i}\sum_{j=1}^{2}\boldsymbol{k}\cdot\left(\frac{\partial \phi_i \boldsymbol{U}_i}{\partial \phi_j}\right)^{(0)} A_j \quad (i = 1,2), \tag{4.5}$$

and on eliminating the amplitudes A_1 and A_2 we find

$$(\sigma - \mathrm{i}\boldsymbol{k}\cdot\boldsymbol{c} + iK_{11})(\sigma - \mathrm{i}\boldsymbol{k}\cdot\boldsymbol{c} + \mathrm{i}K_{22}) = -K_{12}K_{21}, \tag{4.6}$$

where we have written

$$K_{ij} = \boldsymbol{k}\cdot\left[\frac{\partial \phi_i \boldsymbol{U}_i}{\partial \phi_j}\right]^{(0)}. \tag{4.7}$$

The solution of the quadratic equation for σ is

$$\sigma - \mathrm{i}\boldsymbol{k}\cdot\boldsymbol{c} = -\tfrac{1}{2}\mathrm{i}(K_{11} + K_{22}) \mp \tfrac{1}{2}\mathrm{i}[(K_{11} - K_{22})^2 + 4K_{12}K_{21}]^{\frac{1}{2}}, \tag{4.8}$$

from which it may be seen that the condition for an exponentially growing disturbance to exist, that is the condition that there is a positive root for σ, is

$$(K_{11} - K_{22})^2 + 4K_{12}K_{21} < 0. \tag{4.9}$$

Since $\boldsymbol{U}_1$ and $\boldsymbol{U}_2$ and hence also $\boldsymbol{c}$ are vertical vectors we may write

$$K_{ij} = k\cos\theta\left(\frac{\partial \phi_i U_i}{\partial \phi_j}\right)^{(0)}, \quad \boldsymbol{k}\cdot\boldsymbol{c} = kc\cos\theta,$$

where U_i and c are signed quantities, being positive when $\boldsymbol{U}_i$ and $\boldsymbol{c}$ are downward vertical vectors like gravity and negative when upward, and θ is the angle made with

the downward vertical by the wavenumber vector $\boldsymbol{k}$. The condition for instability is then

$$I = \left(\frac{\partial\phi_1 U_1}{\partial\phi_1} - \frac{\partial\phi_2 U_2}{\partial\phi_2}\right)^2 + 4\frac{\partial\phi_1 U_1}{\partial\phi_2}\frac{\partial\phi_2 U_2}{\partial\phi_1} < 0, \tag{4.10}$$

the superscript zero now being regarded as understood.

When this condition is satisfied

$$\sigma = \mp\tfrac{1}{2}k\cos\theta(-I)^{\frac{1}{2}}, \quad c = \frac{1}{2}\left(\frac{\partial\phi_1 U_1}{\partial\phi_1} + \frac{\partial\phi_2 U_2}{\partial\phi_2}\right) \tag{4.11}$$

and

$$\frac{A_2}{A_1} = \frac{\mp i(-I)^{\frac{1}{2}} - \dfrac{\partial\phi_1 U_1}{\partial\phi_1} + \dfrac{\partial\phi_2 U_2}{\partial\phi_2}}{2\dfrac{\partial\phi_1 U_1}{\partial\phi_2}}. \tag{4.12}$$

The difference between the phases of the sinusoidal variations of ϕ_1 and of ϕ_2 lies between 0 and π when $I < 0$.

At the limit $I \uparrow 0$ we have

$$\frac{\partial\phi_1 U_1}{\partial\phi_1} - \frac{\partial\phi_2 U_2}{\partial\phi_2} = \mp 2\left(-\frac{\partial\phi_1 U_1}{\partial\phi_2}\frac{\partial\phi_2 U_2}{\partial\phi_1}\right)^{\frac{1}{2}} \tag{4.13}$$

and

$$\frac{A_2}{A_1} = \pm\left(-\frac{\partial\phi_2 U_2}{\partial\phi_1}\frac{\partial\phi_1 U_1}{\partial\phi_2}\right)^{\frac{1}{2}} \Big/ \frac{\partial\phi_1 U_1}{\partial\phi_2}. \tag{4.14}$$

There are thus two possible forms of neutral disturbance at the boundary of a domain of instability corresponding to the two possible signs on the right-hand side of (4.14). The difference between the phases of the ϕ_1 wave and of the ϕ_2 wave is 0 (corresponding to the positive sign) or π (corresponding to the negative sign) if $\partial\phi_1 U_1/\partial\phi_2$ is positive, and π or 0 if $\partial\phi_1 U_1/\partial\phi_2$ is negative. When the phase difference is π the two types of particle are being separated from each other, whereas when it is 0 the two types of particle are being concentrated in the same regions of space.

When $I > 0$ on the other hand,

$$\sigma = 0, \quad c = \frac{1}{2}\left(\frac{\partial\phi_1 U_1}{\partial\phi_1} + \frac{\partial\phi_2 U_2}{\partial\phi_2}\right) \mp \tfrac{1}{2}I^{\frac{1}{2}}. \tag{4.15}$$

All Fourier components now propagate without change of amplitude, and there are two possible wave speeds, both independent of k, corresponding to different values of the (real) amplitude ratio A_2/A_1.

We note that in the absence of hydrodynamic coupling between the two particle species, i.e. when $\partial U_1/\partial\phi_2$ and $\partial U_2/\partial\phi_1$ are zero, (4.6) reduces to two independent undamped concentration waves propagating vertically with speeds $\partial\phi_1 U_1/\partial\phi_1$ and $\partial\phi_2 U_2/\partial\phi_2$ as would be expected. The possibility of growing modes is connected with the dependence of the mean fall speed of one type of particle on the presence of the other. More specifically, it appears from (4.10) that instability is possible only if $\partial U_1/\partial\phi_2$ and $\partial U_2/\partial\phi_1$ have opposite signs and a product of sufficiently large magnitude.

We have yet to determine whether the condition (4.10) is satisfied for bidisperse systems relevant in practice, but even so it is interesting, and rather surprising, to have established that growing waves exist in principle in a statistically homogeneous dispersion in which particles move under the action of gravity and viscous stresses

only. The possible existence of growing or decaying concentration waves in a bidispersion becomes obvious as soon as it is realized that a spatial variation of concentration of one species causes the mean velocity of the particles of the other species to be non-uniform.

5. Dependence of the growth rate on wavenumber

When the condition (4.10) is satisfied, all Fourier components of the disturbance are amplified and the rate of amplification is proportional to the vertical component of the wavenumber $\boldsymbol{k}$. This is not realistic for very large values of k, and it is necessary now to consider the additional process or effect that causes the expression (4.11) for σ to be invalid at large values of k and that perhaps determines a wavenumber for which the growth rate has a maximum.

As mentioned previously, our assumption that U_1 and U_2 depend only on the local values of ϕ_1 and ϕ_2 will be an accurate approximation only if the spatial gradients of ϕ_1 and ϕ_2 are small, that is, only if k is small. The values of U_1 and U_2 at a point in the dispersion depend in reality on the global configuration of particles, and it is to be expected that, as departures from statistical homogeneity are increased, so the departures of U_1 and U_2 from the values corresponding to those for a homogeneous dispersion with particle concentrations equal to the local values of ϕ_2 and ϕ_2 will increase. For quantitative information we can appeal to a calculation made by Feuillebois (1984) of the mean particle velocity in a dilute monodispersion in which only pairwise interactions are significant and in which the concentration has a vertical variation of the form

$$\phi = \phi_0(1 + A\cos kx). \tag{5.1}$$

This was not an exact calculation, because the distribution of particle pairs was assumed arbitrarily to be uniform for pair separations greater than $2a$, but nevertheless the results should indicate the general magnitude of the effect of concentration variation on the mean particle velocity.

Feuillebois found that

$$U(x) = U_0\{1 - 6.55\phi_0(1 + \alpha A\cos kx) + O(\phi_0^2)\}, \tag{5.2}$$

where α is a function of ka only (a being the particle radius) which varies between the limits $\alpha \to 1$ as $ka \to 0$, corresponding to $(U - U_0)/U_0$ having the 'local' value expected for the assumed pair-distribution function, viz. -6.55 times the local concentration, and $\alpha \to 0$ as $ka \to \infty$, corresponding to $(U - U_0)/U_0$ being equal to -6.55 times the average of the concentration over a neighbourhood of x. For $ka \ll 1$ Feuillebois finds the asymptotic relationship

$$\alpha \sim 1 - 0.67\, ka,$$

which gives α correct to within 10 % for values of ka up to about 0.65 and shows that the range of variation of U as a function of x when $ka = 0.65$ is only 0.56 of that when $ka = 0$.

The effect of increasing the wavenumber of a sinusoidal variation of concentration in a monodispersion is thus to reduce the range of variation of mean particle velocity as a function of position, and to reduce it to zero as $ka \to \infty$. The same may be expected to be true of a bidispersion. This is a stabilizing influence in a bidispersion with sinusoidal variations of the two concentrations, because without spatial variations of the mean particle velocities there can be no amplification of the disturbance. The

linear dependence of the growth rate σ on wavenumber k found in (4.11) will thus be modified at non-small values of ka (where $a = \frac{1}{2}(a_1 + a_2)$) when the influence of spatial variations of ϕ_1 and ϕ_2 on the mean particle velocities is taken into account, and there will evidently be a value of ka, $k_m a$ say, for which σ is a maximum and another value, $k_c a$ say, at which $\sigma = 0$. No theoretical estimates of $k_m a$ and $k_c a$ are available, but Feuillebois's calculation for a monodispersion suggests that $k_m a < 1$ and $k_c a$ is of order unity.

The effect of the diffusion term (4.2) which has not been taken into account in the above perturbation analysis would likewise increase, and ultimately become dominant, as $ka \to \infty$. The magnitude of the ratio of this neglected diffusion term to the retained 'convection' terms in (4.3) may be estimated as $k^2 D_0/kU_0$, where U_0 is representative of the mean particle speeds (e.g. $\frac{1}{2}(|U_1| + |U_2|)$). The representative diffusivity D_0 is the sum of the Brownian diffusivity, which is quite negligible for particles as large as those listed in table 1, and the hydrodynamic diffusivity associated with fluctuations in the velocity of a particle due to changes in the configuration of neighbouring particles. The value of this latter contribution is not known with certainty, but is likely to be of order $a_i |U_i|$ for the i-type particles, provided the total particle concentration is not near maximum packing, or aU_0 if we may assume the two particle radii and mean speeds to be not greatly different. Thus the ratio of the neglected to the retained term is of order ka in general and the neglect is justified provided $ka \ll 1$.

Diffusion processes normally have a stabilizing influence on small disturbances. However, hydrodynamically driven diffusion of sedimenting particles has some unusual features, and the effect on small disturbances depends on the relative magnitudes of the diagonal and off-diagonal elements of the diffusivity matrix, about which very little information is available. Whether the influence is stabilizing or destabilizing is not an important question for disturbances with non-horizontal wavenumber vectors, because if $ka \ll 1$ the convective processes investigated in §4 are dominant and if $ka = O(1)$ non-local effects of the kind described above modify the values of the mean particle velocities and ensure stability. But for disturbances with horizontal wavenumber vectors the question is of some consequence because the convection terms in (4.3) are then identically zero and the growth or decay of disturbances for which $ka \ll 1$ is determined by hydrodynamic diffusion processes alone.

It may be admitted here that for a long time we were misled by the predominantly vertical and cylindrical character of the structures formed in a sedimenting bidispersion, as reported by Weiland and his colleagues and as observed in our own initial experiments. This led us to infer that the dispersion is unstable only to disturbances with horizontal wavenumbers, and to seek an explanation for the instability in the effect of the diffusion term, and specifically in the effect of the cross-diffusivities. However, our later experiments showed that the structures that emerge spontaneously from a well-mixed dispersion are not vertical or column-like in every case and that, even when streaming columns do form, they are preceded by drop-like concentrations of particles and so are likely to be caused by secondary bulk-buoyancy effects (see for example the photographs in figures 2*a–e*). Guided by these further observations, we made a closer study of the possibility that the convective terms in (4.3) cause growth of small disturbances with non-horizontal wavenumbers and found enough evidence, to be described in §6, to persuade ourselves that the condition (4.10) is indeed satisfied for certain ranges of values of λ, γ, ϕ_1 and ϕ_2. The question whether hydrodynamic diffusion causes disturbances with

horizontal wavenumber vectors to grow, although interesting theoretically, thus seems not to be relevant to the explanation of the formation of the observed structures and will not be pursued here.

6. Satisfaction of the condition (4.10) for instability

Only a limited amount of information about the dependence of the mean particle velocities U_1 and U_2 in a homogeneous dispersion on the four parameters ϕ_1, ϕ_2, λ, γ is available. In this section we try to use this information to determine the sign of the quantity

$$I = \left(\frac{\partial \phi_1 U_1}{\partial \phi_1} - \frac{\partial \phi_2 U_2}{\partial \phi_2}\right)^2 + 4\phi_1 \phi_2 \frac{\partial U_1}{\partial \phi_2}\frac{\partial U_2}{\partial \phi_1} \tag{6.1}$$

for specified ranges of values of ϕ_1, ϕ_2, λ and γ. Exponentially growing disturbances exist only if $I < 0$. It will be recalled that U_1 and U_2 are defined as the vertical components of the mean particle velocities and so may have either sign.

We note first one or two immediate general results. As $\phi_1 \to 0$ or $\phi_2 \to 0$ we have

$$I \to \left(\frac{\partial \phi_1 U_1}{\partial \phi_1} - \frac{\partial \phi_2 U_2}{\partial \phi_2}\right)^2,$$

which is positive definite, showing that all bidispersions are stable when either ϕ_1 or ϕ_2 is sufficiently small. A necessary condition for instability is that the change in the mean velocity of particles of type i due to the addition of some particles of the other type should have opposite senses when $i = 1$ and $i = 2$. A special case for which this condition is not satisfied is $\lambda = 1$, $\gamma = 1$, for which U_1 and U_2 are equal and depend only on $\phi_1 + \phi_2$, showing the expected stability for two identical species of particles.

Dilute dispersions

When $\varphi = \phi_1 + \phi_2 \ll 1$ we may write

$$\left.\begin{aligned} U_1 &= U_{10}\{1 + S_{11}\phi_1 + S_{12}\phi_2 + O(\phi^2)\} \\ U_2 &= U_{20}\{1 + S_{21}\phi_1 + S_{22}\phi_2 + O(\phi^2)\}, \end{aligned}\right\} \tag{6.2}$$

where U_{10} and U_{20} ($= \gamma\lambda^2 U_{10}$) are the vertical components of the velocities of isolated particles of types 1 and 2. The sedimentation coefficients S_{11}, S_{22}, S_{12}, S_{21} depend on the hydrodynamic interactions between pairs of particles, and their values are known from either observation or theory for a variety of conditions. S_{11} and S_{22} both represent the sedimentation coefficient for a monodispersion, which is widely accepted on empirical grounds as having a value within about 20 % of -5.5 for rigid spheres with diameters between 2 μm and 100 μm. (At small Péclet number the value -6.55 calculated for a uniform pair-distribution function is well established, but for larger particles there is some theoretical uncertainty about the effect of possible departures of the pair-distribution function from uniformity in a monodispersion.) The coupling sedimentation coefficients S_{12} and S_{21} have recently been calculated for a number of values of λ and γ both for large and for small values of the Péclet number (Batchelor 1982; Batchelor & Wen 1982), and the results for large Péclet number – the condition relevant here – are set out in tables 1 and 2 and figures 6 and 7 in the second of these two papers; none of these results has yet been checked experimentally.

As already mentioned, $I > 0$ when either ϕ_1 or ϕ_2 is sufficiently small. No rigorous deductions about change of the sign of I from positive to negative as ϕ_1

and ϕ_2 increase from zero may be made by use of the expressions (6.2), because I can change sign only when terms of different algebraic order in ϕ are numerically comparable in magnitude. Nevertheless the expressions (6.2) indicate the trends of the functions U_1 and U_2, and allow reasonable conjectures about the circumstances in which I changes sign.

Consider first the particle system with the properties

$$\lambda = 1, \quad \gamma = -1, \quad U_{20} = -U_{10}, \tag{6.3}$$

and put

$$U_1 = U_{10} F_1(\phi_1, \phi_2), \quad U_2 = U_{20} F_2(\phi_1, \phi_2) = U_{20} F_1(\phi_2, \phi_1). \tag{6.4}$$

Then when $\phi_1 = \phi_2$ we have from the symmetry of the system

$$F_1 = F_2, \quad \frac{\partial F_1}{\partial \phi_1} = \frac{\partial F_2}{\partial \phi_2}, \quad \frac{\partial F_1}{\partial \phi_2} = \frac{\partial F_2}{\partial \phi_1} \tag{6.5}$$

and consequently

$$I = 4U_{10}^2 \left\{ \left(\frac{\partial \phi_1 F_1}{\partial \phi_1} \right)^2_{\phi_2 = \phi_1} - \phi_1^2 \left(\frac{\partial F_1}{\partial \phi_2} \right)^2_{\phi_2 = \phi_1} \right\}. \tag{6.6}$$

Now the numerical data for a dilute dispersion mentioned above show that

$$S_{11} \approx -5.5, \quad S_{12} = -2.4,$$

whence we see from (6.2) that

$$\left(\frac{\partial \phi_1 F_1}{\partial \phi_1} \right)_{\phi_2 = \phi_1} = 1 - 13.4\phi_1 + O(\phi^2), \quad -\left(\phi_1 \frac{\partial F_1}{\partial \phi_2} \right)_{\phi_2 = \phi_1} = 2.4\phi_1 + O(\phi^2) \tag{6.7}$$

when ϕ_1 and ϕ_2 are small.

These two linear functions of ϕ_1 are shown as broken lines in figure 8. For comparison we also show $(\partial \phi_1 F_1 / \partial \phi_1)_{\phi_2 = 0}$ for a case in which

$$F_1(\phi_1, 0) = (1 - \phi_1)^{5.5}, \tag{6.8}$$

which is a good fit, over the whole range of values of ϕ_1, to the observations of mean velocity of particles of radius 1.55 μm in a monodispersion made by Buscall *et al.* (1982). The difference between this curve and the straight line that is tangent to it at the origin is small until ϕ_1 exceeds about 0.05, and it seems likely that the same is true of $\partial \phi_1 F_1 / \partial \phi_1$ for a bidisperse system when ϕ_2 is also small. Since F_1 has a very small value at maximum packing of the particles, the integral of $\partial \phi_1 F_1 / \partial \phi_1$ over the whole range of values of ϕ_1 for given ϕ_2 is approximately zero. It is therefore very likely that $(\partial \phi_1 F_1 / \partial \phi_1)_{\phi_2 = \phi_1}$ is negative for some (large) values of ϕ_1. The full curves in figure 8 representing $(\partial \phi_1 F_1 / \partial \phi_1)_{\phi_2 = \phi_1}$ and $-(\phi_1 \partial F_1 / \partial \phi_2)_{\phi_2 = \phi_1}$ have been drawn heuristically in conformity with these requirements. Intersection of the two curves seems inevitable, and according to (6.6) I is decreasing through zero at this point of intersection. This is the basis of our belief that the condition for instability is satisfied for some values of ϕ_1 and ϕ_2 when $\lambda = 1$, $\gamma = -1$.

If this intersection of the curves is accepted, there is a neutral stability point at a common value of ϕ_1 and ϕ_2 which appears to be roughly 0.09. The difference between the phases of the waves in ϕ_1 and in ϕ_2 at this neutral stability point is zero according to (4.13) and (4.14), because $(\partial \phi_1 F_1 / \partial \phi_1)_{\phi_2 = \phi_1}$ is positive and $(\phi_1 \partial F_1 / \partial \phi_2)_{\phi_2 = \phi_1}$ is negative at $\phi_1 = \phi_2 = 0.09$. This is an important conclusion with a bearing on the observed particle structures, to which we shall refer in the next section. At common

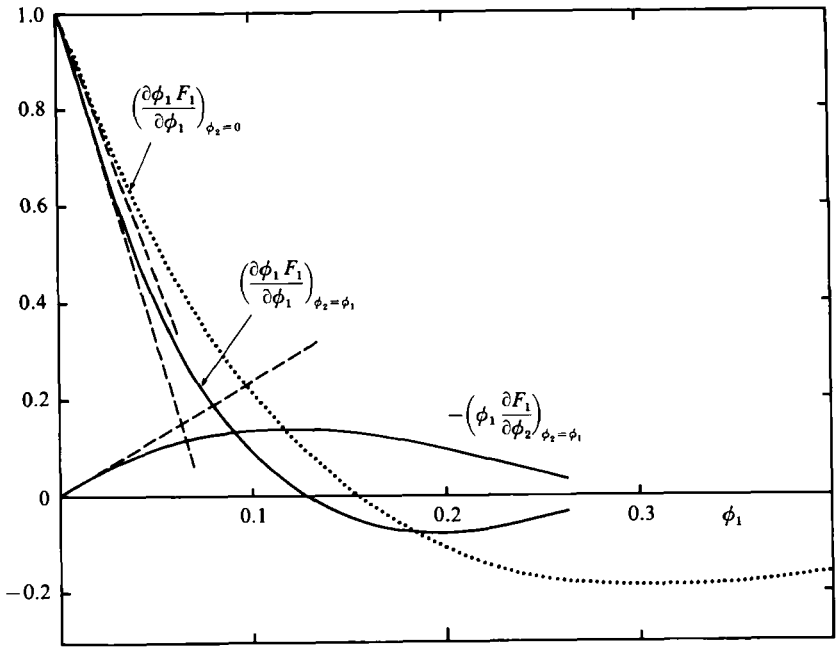

FIGURE 8. Functions relevant to the instability criterion for a bidispersion for which $\lambda = 1, \gamma = -1$. The dotted curve for $(\partial\phi_1 F_1/\partial\phi_1)_{\phi_2=0}$ is empirical. The three dashed lines are calculated asymptotes for $\phi_1 \ll 1$. The two continuous curves are conjectural. The growth rate of a small disturbance first becomes positive, as ϕ_1 and ϕ_2 are increased together from zero, at the value of ϕ_1 at which the two continuous lines cross.

values of ϕ_1 and ϕ_2 above about 0.09, $I < 0$ and growing modes exist. On further increase of ϕ_1 and ϕ_2, F_1 becomes small and I presumably decreases to a minimum and later increases. Without more information about the dependence of F_1 on ϕ_1 and ϕ_2 it is impossible to say whether the quantities $(\partial\phi_1 F_1/\partial\phi_1)_{\phi_2=\phi_1}$ and $(\phi_1\partial F_1/\partial\phi_2)_{\phi_2=\phi_1}$ again have equal magnitude at some value of ϕ_1 and ϕ_2 less than that for close packing of the particles (viz. $\phi_1 = \phi_2 \approx 0.32$). If there is a second neutral stability point, the difference between the phases of the waves in ϕ_1 and ϕ_2 is π there if $(\partial\phi_1 F_1/\partial\phi_1)_{\phi_2=\phi_1}$ is negative and 0 if it is positive. The wave speed of both neutral and amplified disturbances is zero when $\phi_1 = \phi_2$.

Similar considerations apply to the particle system defined by (6.3) with *unequal* values of ϕ_1 and ϕ_2, although now we no longer have available the relations (6.5). In place of (6.6) we have

$$I = U_{10}^2\left\{\left(\frac{\partial\phi_1 F_1}{\partial\phi_1}+\frac{\partial\phi_2 F_2}{\partial\phi_2}\right)^2 - 4\phi_1\phi_2\frac{\partial F_1}{\partial\phi_2}\frac{\partial F_2}{\partial\phi_1}\right\}, \tag{6.9}$$

and in place of (6.7)

$$\left.\begin{aligned}\frac{\partial\phi_1 F_1}{\partial\phi_1} &\approx 1-11.0\phi_1-2.4\phi_2, \quad \phi_1\frac{\partial F_1}{\partial\phi_2} \approx -2.4\phi_1,\\ \frac{\partial\phi_2 F_2}{\partial\phi_2} &\approx 1-11.0\phi_2-2.4\phi_1, \quad \phi_2\frac{\partial F_2}{\partial\phi_1} \approx -2.4\phi_2,\end{aligned}\right\} \tag{6.10}$$

when ϕ_1, $\phi_2 \ll 1$. If we use these expressions regardless of the restrictions on ϕ_1 and ϕ_2, we find that I decreases through zero as ϕ_1 increases, with α fixed, through a value given by

$$\phi_1 = \frac{2}{13.4(1+\alpha)+(23.0\alpha)^{\frac{1}{2}}}, \quad \alpha = \frac{\phi_2}{\phi_1}. \tag{6.11}$$

When $\alpha = 1$ this recovers the value of ϕ_1 given by the intersection of the two broken lines in figure 8 (viz. 0.063); and when $\alpha \neq 1$, either ϕ_1 or ϕ_2 is less than 0.063 at this neutral point and the other is greater than 0.063.

The dilute-dispersion formulae (6.2) may be used to get an indication of whether the dispersion is unstable in other cases. Consider for instance the particle pair given by $\lambda = 1$, $\gamma = -2$, values which are close to those for Weiland, Fessas & Ramarao's system A, listed in table 1. We have here

$$S_{12} = -2.26, \quad S_{21} = -2.45.$$

The term outside the brackets in (6.1) does have the negative sign required for instability, and we find that the first neutral point is given roughly by

$$3 - 15.9\phi_1 - 24.3\phi_2 = (44.3\phi_1\phi_2)^{\frac{1}{2}}. \tag{6.12}$$

When $\phi_1 = \phi_2$ this yields $\phi_1 = 0.064$.

Likewise for $\lambda = 0.5$, $\gamma = -5$, which approximates to the particle pair in Fessas & Weiland's system A, we have

$$S_{12} \approx -5.0, \quad S_{21} \approx -2.2,$$

and the relation specifying the first neutral point crudely is

$$2.25 - 13.8\phi_1 - 18.8\phi_2 = (55\phi_1\phi_2)^{\frac{1}{2}}. \tag{6.13}$$

When $\phi_1 = \phi_2$ this gives $\phi_1 = 0.056$.

Finally, we note from table 1 in the paper by Batchelor & Wen (1982) that when $\gamma > 0$ the coefficients S_{12} and S_{21} are both negative for all combinations of values of λ and γ except when $\gamma \gg 1$. It appears that the term outside the brackets in (6.1) is always positive when γ is positive and of order unity, thus precluding the possibility of finding instability from the dilute-dispersion formulae. However, it may be that, when $\phi_1 + \phi_2$ is fairly large, the addition of more particles of either type would bring the dispersion closer to maximum packing and each mean particle velocity closer to a common intermediate value, corresponding to $\partial U_1/\partial\phi_2$ and $\partial U_2/\partial\phi_1$ having *opposite* signs. Consequently the possibility of instability when $\gamma > 0$ may exist at large values of ϕ_1 and ϕ_2.

The case $\lambda \ll 1$

When the spheres of one species (type 2 say) are much smaller than those of the other species, the hydrodynamic interaction of the two species takes a simpler form. The physical approximations that are possible in this case have been considered previously in the context of dilute bidispersions (Batchelor 1982) but are equally applicable at other concentrations.

The medium outside the larger spheres now behaves approximately as a continuum, on the scale of the large spheres, with mean density

$$\rho_0 + \psi(\rho_2 - \rho_0), \quad \text{where } \psi = \frac{\phi_2}{1-\phi_1},$$

and an effective viscosity $\mu f(\psi)$, where μ is the fluid viscosity and ψ is the fraction of the volume outside the larger spheres that is occupied by the smaller type-2 spheres. The mean velocity of the larger type-1 spheres is thus given approximately by the formula for a monodispersion, and we may write

$$U_1 \approx U_{10} B(\phi_1) \frac{1-\gamma\psi}{f(\psi)}. \tag{6.14}$$

Here $B(\phi_1)$ is the mobility function specifying the dependence of the settling velocity in a homogeneous monodispersion on the volume fraction of the particles, and $U_{10}(1-\gamma\psi)/f$ is the velocity of an isolated type-1 sphere of density ρ_1 in a fluid of density $\rho_0+\psi(\rho_2-\rho_0)$ and viscosity μf. Empirical information about the positive functions $B(\phi_1)$ and $f(\psi)$ is available.

The smaller type-2 spheres on the other hand are dispersed with volume fraction ψ in a pure fluid of density ρ_0 and viscosity μ, and the main effect of the presence of the larger type-1 spheres is to generate a mean velocity $-U_1\phi_1/(1-\phi_1)$ in the mixture of pure fluid and small type-2 spheres. Thus the mean velocity of the type-2 spheres is approximately

$$U_2 = U_{20} B(\psi) - \frac{\phi_1 U_1}{1-\phi_1}, \tag{6.15}$$

and $U_{20} = \gamma\lambda^2 U_{10}$.

On substituting these approximate expression (6.14) and (6.15) into (6.1) we find, after some working, that

$$\frac{I}{U_{10}^2} = \left[C(\psi)\left\{\frac{B(\phi_1)}{1-\phi_1} + \phi_1 B'(\phi_1)\right\} - \gamma\lambda^2\{B(\psi)+\psi B'(\psi)\}\right]^2 - 4\gamma\lambda^2 \frac{\phi_1\psi}{1-\phi_1} B(\phi_1) B(\psi) C'(\psi), \tag{6.16}$$

where $B'(\phi_1) = \mathrm{d}B/\mathrm{d}\phi_1$ and $C(\psi) = (1-\gamma\psi)/f(\psi)$. Only the squared term in (6.16) survives in the limit $\lambda \to 0$, showing that $I > 0$ for a certain small range of values of λ. Moreover, the second (unsquared) term in (6.16) is non-negative when $\gamma C'(\psi) \leqslant 0$. This condition is satisfied when $0 \leqslant \gamma\psi \leqslant 1$, suggesting that the expression (6.16) is positive for a larger range of (small) values of λ when $\gamma\psi$ lies within this range.

Thus the dispersion is stable when the spheres of one species are much smaller than those of the other species, for any value of the density ratio γ and for any values of the volume fractions ϕ_1 and ϕ_2. The condition on λ for stability is likely to be less restrictive for positive values of γ of order unity.

7. The relation between the theory and observations

It remains now to consider the extent to which the theoretical results obtained in §§4, 5, 6 are in accord with the observations described in §§2, 3.

The main accomplishment of the theory is of course that it provides an explanation for the observed occurrence of finite disturbances to a statistically homogeneous bidispersion under some, but not all, conditions. The explanation involves only the movement of the particles through fluid due to gravity and hydrodynamic interaction of the particles, the same two processes that alone are believed to be at work in the dispersions observed in the laboratory. However, there is more than one way in which these two processes may be represented by equations involving averaged quantities, and a decisive test of the theory requires a quantitative comparison with the

observations. This is beset by difficulties, both in the calculations and in the experiments, and we have not been able to achieve precision or completeness in the comparison.

We compare the theory and observations under two headings, first the conditions for instability and second the properties of the structures that arise spontaneously in a homogeneous bidispersion.

The conditions for instability

The stability of the bidispersion to small disturbances depends on the values of the four parameters $\lambda, \gamma, \phi_1, \phi_2$. There is presumably a relation between these parameters representing a boundary in the four-dimensional space which separates a region of instability from a region in which disturbances propagate as waves without change of form or amplitude. Almost all the observational evidence concerning the critical conditions is summarized by figures 6 and 7, in which the stability boundary is determined approximately, as a band rather than as a line. Many more such figures will need to be compiled before the complete shape of the stability boundary becomes clear. Nevertheless, the existence of a stability boundary is well established by the observations and some features of its shape can be identified.

According to the theory, the relation specifying critical conditions is $I = 0$, where I is defined in (6.1), and the bidispersion is unstable on the side of the boundary on which $I < 0$. We saw that I approaches a positive limit as either $\phi_1 \to 0$ or $\phi_2 \to 0$, indicating stability near the ϕ_1 and ϕ_2 axes in figure 6, in accordance with the data. The quantity I involves the mean particle velocities U_1 and U_2, and at present we are able to calculate U_1 and U_2 as functions of $\lambda, \gamma, \phi_1, \phi_2$ accurately only for small values of ϕ_1 and ϕ_2. The trend of I as a function of ϕ_1 and ϕ_2 for a dilute bidispersion suggests that I decreases to zero as ϕ_1 or ϕ_2 increases, for certain values of λ and γ. This suggestion is clearest for the case $\lambda = 1$, $\gamma = -1$, for which I becomes zero when ϕ_1 and ϕ_2 are increased together to a value roughly equal to 0.09 (the critical condition $I = 0$ being attained when the two conjectural unbroken lines in figure 8 cross). The point $\phi_1 = 0.09$, $\phi_2 = 0.09$ will be seen to lie within the band indicating critical conditions in figure 6. The dependence of I on ϕ_1 and ϕ_2 for the same dilute dispersion also suggests that I becomes zero, as ϕ_1 say is increased with ϕ_2 fixed, at a value of ϕ_1 which is larger for smaller values of ϕ_2, again in accordance with the data in figure 6. A generally similar shape of the stability boundary near the origin of the (ϕ_1, ϕ_2)-plane is suggested by the dilute-dispersion formulae for other values of λ and γ provided $\gamma < 0$, and this is consistent with the limited number of observations made on such systems. There is however no suggestion from the dilute-dispersion formulae that I becomes negative as ϕ_1 and ϕ_2 are increased from zero when $\gamma > 0$; if I does become negative in this case, it will be at larger values of ϕ_1 and ϕ_2 than in cases for which $\gamma < 0$. Figure 7 does in fact show the occurrence of instability when $\phi_1 = \phi_2 = 0.15$ at some positive values of γ.

We saw from a consideration of a heuristic model of a bidispersion for which $\lambda \ll 1$ (or $\lambda \gg 1$) that $I > 0$ in such cases regardless of the values of γ, ϕ_1 and ϕ_2. This is in accordance with the position of the stability boundary in figure 7 for systems for which $\phi_1 = \phi_2 = 0.15$. Figure 7 shows that the range of values of λ for which there is instability is zero when $\gamma = 1$, and is approximately $\frac{1}{3} < \lambda < 3$ when $\gamma = 0$ and a little larger when $\gamma = -1$, a trend which is consistent with the dependence of (6.16) on γ noted at the end of §6. Bidispersions in which one type of particle is much smaller than the other occur often in practice, so it is useful to know that, according to the theory, they are always stable. The observed stability of a mixture of any two sizes

of particles made of the same material when $\phi_1 = \phi_2 = 0.15$ is also noteworthy from a practical viewpoint, and it would be useful to know if the same is true at other concentrations.

In summary, the rather limited quantitative predictions of the theory are all consistent with the observations of the critical conditions for instability.

The properties of the emergent structures

Some comparison of theory and observation is also possible under this heading if we may assume that the observed structures are a finite-amplitude development from the normal-mode small disturbances for which the growth rates are close to their maximum. With this assumption the size, shape, degree of particle separation, and time of formation of the observed structures should reflect the calculated properties of the normal modes that become dominant by the usual process of selective amplification. However, a simple correspondence of the observed structures and the dominant normal-mode disturbance cannot be expected, for a number of reasons.

There is firstly the difficulty that the instability lies in the spatial distribution of averaged properties of the dispersion, in particular the particle concentration, which has not been observed directly. We have observed discrete particles, whose positions and motions in one realization reflect the mean properties of a disturbance only in a ragged manner. Secondly, this instability is not related to the existence of boundaries, and small disturbances in different parts of the dispersion may be amplified independently, giving rise to a confusing concentration distribution without long-range order. Thirdly, the growth of a disturbance to the concentration distribution generates bulk density variations and vertical convection currents which soon become stronger than the vertical velocities in the homogeneous dispersion (for instance, the fall speed of a sphere of the mixture of radius 20 times the radius of monodisperse particles becomes comparable with the mean speed of the particles relative to local zero-volume-flux axes when the excess volume fraction of the particles in the sphere is only 0.0025 of the overall volume fraction), and these currents deform the growing disturbances. A fourth reason for expecting the form of the emergent structures to be irregular is the deduction from the theory that all Fourier components of a disturbance with equal vertical components of the wavenumber vector have the same growth rate and that although the growth rate is a maximum, for given wavenumber magnitude, when the wavenumber vector is vertical it is a weakly defined maximum. All these difficulties make it a good deal easier to decide whether structures have formed than to say what they look like. It is not surprising that we do not see sinusoidal variations of particle concentration.

We have given in separate columns of table 4 our rough estimates of the optical contrast, the general shape (as one of four types), the horizontal width d, and the time of evolution τ (taken as being the time for the onset of visible bulk convective motions) of the structures observed in a large number of unstable systems for which $\lambda = 1$ and $\gamma = -1$.

Our observations of the degree of optical contrast in the structures formed in systems for which $\lambda = 1$, $\gamma = -1$, may be summarized by the statement that the contrast is poor for the lowest value of $\phi_1 + \phi_2$ at which a system is unstable and becomes stronger as $\phi_1 + \phi_2$ is increased (see figure 6). Optical contrast is a measure of the separation of the two particle species, and the instability evidently causes a degree of particle separation which is stronger when $\phi_1 + \phi_2$ is larger. The bulk convective motions that are generated by gravity acting on spatial variations of concentration do not change the particle concentration in a material element of the

mixture, so that the separation of the two particle species must occur in the regime of exponentially growing small disturbances.

The observed dependence of the particle separation on $\phi_1+\phi_2$ is in fact similar to what the linear instability theory predicts. It will be recalled from §4 that there are two possible forms of neutral disturbance at the boundary of a domain of instability, the difference between the phases of the sinusoidal variations of the concentrations of the two particle species being 0 in one case and π in the other. We also showed in §6 from dilute-dispersion calculations that, for the symmetrical system given by $\lambda = 1$, $\gamma = -1$, $\phi_1 = \phi_2$, the quantity I is positive when $\phi_1 = \phi_2 = 0$ and decreases through zero as ϕ_1 and ϕ_2 increase through a value of about 0.09, in accordance with the observations shown in figure 6, and that the phase difference is zero at the point where $I = 0$ and increases from zero as ϕ_1 and ϕ_2 are increased from 0.09. Thus the theory predicts minimum separation of the two particle species and minimum optical contrast in the emergent structures at $\phi_1 = \phi_2 \approx 0.09$ – and, from continuity, on the whole of the stability boundary shown in figure 6 – and increasingly strong contrast as the point representing the system in the (ϕ_1, ϕ_2)-plane moves away from the stability boundary.

The observed dependence of the contrast in the structures on the values of λ and γ for systems for which $\phi_1 = \phi_2 = 0.15$ is recorded in table 5. It will be seen that the contrast is generally poor close to the stability boundary, and becomes stronger as the system point moves away from the stability boundary in the (λ, γ)-plane shown in figure 7. This is what would be expected from the theory if, as seems probable on geometrical grounds, the stability boundaries shown in figures 6 and 7 are two sections of a connected surface in the space of λ, γ, ϕ_1, ϕ_2 on which $I = 0$ and the difference between the phases of the sinusoidal variations in the two particle concentrations is zero.

The shapes of the structures observed to form in unstable systems for which $\lambda = 1$, $\gamma = -1$ are given in the column of table 4 headed 'type', and, as noted in §3 and figure 6, there is a tendency for systems with smaller values of the total volume fraction $\phi_1+\phi_2$ to yield vertical streams or columns and systems with larger values to yield blobs. We cannot account for this tendency. The linear instability theory tells us only that Fourier components of an initial infinitesimal disturbance are amplified at a rate which depends on their wavenumber vector, whereas the observed structures depend also on the interaction of Fourier components and on the bulk convection that develops when the disturbance amplitude is only modest. In some way these latter processes evidently generate convective structures with characteristic shapes.

The values of the horizontal width of the structures at 20 s after cessation of mixing range from $d = 21a$ to $d = 67a$ (see table 4), and tend to be larger for larger values of $\phi_1+\phi_2$. It was noted in §3 that the blob-like structures with good particle separation that tend to form at the larger values of $\phi_1+\phi_2$ increase in average size by a process of coalescence associated with the bulk convective motions, and that the rate of coalescence increases with $\phi_1+\phi_2$. On the other hand the horizontal width of the column-like structures did not change much during this interval of 20 s. If we notionally set aside the observations of d in all those cases in table 4 where the structure 'type' is B or BC and the 'contrast' is G, on the grounds that these values of d are influenced by bulk convection, we find that the values of d are much more uniform and with one exception lie in the range $21a$ to $31a$.

We may now consider the relation between this characteristic lengthscale of the observed structures and the lengthscale predicted by the linear instability theory.

The lengthscale of the visible finite-amplitude disturbance is probably a measure in part of the wavelength of the sinusoidal small disturbances that grow most rapidly and in part of the distance normal to the wavenumber vector over which an amplified small disturbance is coherent. However, bulk convection sets in at quite small values of the amplitude of a growing disturbance and is likely to limit coherence to distances comparable with the wavelength, in which event the wavelength of the growing disturbance determines the lengthscale of the emergent structures. Thus we may tentatively identify the observed lengthscale with the wavelength of the sinusoidal disturbance with maximum growth rate, which was denoted by $2\pi/k_m$ in §5. If we take $d = 26a$, this gives $k_m a = 0.24$. The theory is able to say about $k_m a$ only that the dependence of U_1 and U_2 on non-local values of the particle concentrations has a stabilizing influence which becomes stronger as the wavenumber increases and that $k_m a$ is likely to be less than unity.

The observed values of the time of evolution τ of the convective structures given in table 4 range from $20a_1/|U_{10}|$ to $74a_1/|U_{10}|$, and there appears to be a tendency for τ to be larger for larger common values of ϕ_1 and ϕ_2. Now the time τ may be regarded as a sum of a few e-folding times of the fastest-growing sinusoidal disturbance and the time required for bulk buoyancy forces to develop visible collective convection of particles following the creation of spatial variations of the particle concentration. Rough estimates of this latter response time show that it is usually quite small. The non-dimensional e-folding time of the dominant disturbance is given by (4.11) as

$$\left(\frac{|U_{10}|}{\sigma a_1}\right)_{k=k_m} = \frac{2}{k_m a}\frac{|U_{10}|}{(-I)^{\frac{1}{2}}},$$

and inspection of the curves in figure 8 suggests that $(-I)^{\frac{1}{2}}/|U_{10}|$ is roughly 0.2 when ϕ_1 and ϕ_2 are equal and lie in the range 0.1–0.2. If we now take from the experiments the estimate $k_m a \approx 0.24$, we obtain 40 for the non-dimensional e-folding time of the disturbance which is to be identified with $\tau|U_{10}|/a$. The number 40 is of the same order of magnitude as the values of $\tau|U_{10}|/a$ observed for those systems listed in table 4 that have roughly equal values of ϕ_1 and ϕ_2. It is impossible to say more without more information about the numerical values of U_1 and U_2 as functions of ϕ_1 and ϕ_2.

We may conclude that there is a small measure of agreement, and no conflict, between the observed properties of the emergent structures and our linear instability theory.

We thank Professor A. Acrivos of Stanford University for drawing our attention several years ago to the published observations of structure formation in bidispersions and Professor R. H. Weiland of Clarkson College for kindly showing us some of his additional unpublished data on structure formation.

REFERENCES

Batchelor, G. K. 1982 Sedimentation in a dilute polydisperse system of interacting spheres. Part 1. General theory. *J. Fluid Mech.* **119**, 379–408.

Batchelor, G. K. & Wen, C.-S. 1982 Sedimentation in a dilute polydisperse system of interacting spheres. Part 2. Numerical results. *J. Fluid Mech.* **124**, 495–528.

Buscall, R., Goodwin, J. W., Ottewill, R. H. & Tadros, T. F. 1982 The settling of particles through Newtonian and non-Newtonian media. *J. Colloid Interface Sci.* **85**, 78–86.

Fessas, Y. P. & Weiland, R. H. 1981 Convective solids settling induced by a buoyant phase. *AIChEJ.* **27**, 588–592.

FESSAS, Y. P. & WEILAND, R. H. 1982 Convective solids settling induced by a buoyant phase – a new method for the acceleration of thickening. *Resources & Conserv.* **9**, 87–93.

FESSAS, Y. P. & WEILAND, R. H. 1984 The settling of suspensions promoted by rigid buoyant particles. *Intl J. Multiphase Flow* **10**, 485–507.

FEUILLEBOIS, F. 1984 Sedimentation in a dispersion with vertical inhomogeneities. *J. Fluid Mech.* **139**, 145–171.

KYNCH, G. J. 1952 A theory of sedimentation. *Trans. Faraday Soc.* **48**, 166–176.

WEILAND, R. H., FESSAS, Y. P. & RAMARAO, B. V. 1984 On instabilities arising during sedimentation of two-component mixtures of solids. *J. Fluid Mech.* **142**, 383–389.

WEILAND, R. H. & MCPHERSON, R. R. 1979 Accelerated settling by addition of buoyant particles. *Ind. Engng Chem. Fundam.* **18**, 45–49.

WHITMORE, R. L. 1955 The sedimentation of suspensions of spheres. *Brit. J. Appl. Phys.* **6**, 239–245.